Biochimica et Biophysica Acta 1823 (2012) 335–347

Contents lists available at SciVerse ScienceDirect

Biochimica et Biophysica Acta

journal homepage: www.elsevier.com/locate/bbamcr

Bcl2 at the endoplasmic reticulum protects against a Bax/Bak-independent paraptosis-like cell death pathway initiated via p20Bap31

Hannah M. Heath-Engel, Bing Wang, Gordon C. Shore *

Department of Biochemistry and Goodman Cancer Research Center, McGill University, Montréal QC Canada H3G 1Y6

ARTICLE INFO

Article history:
Received 1 August 2011
Received in revised form 29 November 2011
Accepted 30 November 2011
Available online 8 December 2011

Keywords:
Bap31
Bcl-2
Apoptosis
Paraptosis
Vacuolization
Calcium

ABSTRACT

Bap31 is an integral ER membrane protein which functions as an escort factor in the sorting of newly synthesized membrane proteins within the endoplasmic reticulum (ER). During apoptosis signaling, Bap31 is subject to early cleavage by initiator caspase-8. The resulting p20Bap31 (p20) fragment has been shown to initiate proapoptotic ER-mitochondria Ca^{2+} transmission, and to exert dominant negative (DN) effects on ER protein trafficking. We now report that ectopic expression of p20 in E1A/DNp53-transformed baby mouse kidney epithelial cells initiates a non-apoptotic form of cell death with paraptosis-like morphology. This pathway was characterized by an early rise in ER Ca^{2+} stores and massive dilation of the ER/nuclear envelope, dependent on intact ER Ca^{2+} stores. Ablation of the *Bax/Bak* genes had no effect on these ER/nuclear envelope transformations, and delayed but did not prevent cell death. ER-restricted expression of Bcl2 in the absence of Bax/Bak, however, delayed both ER/nuclear envelope dilation and cell death. This prosurvival role of Bcl2 at the ER thus extended beyond inhibition of Bax/Bak, and correlated with its ability to lower ER Ca^{2+} stores. Furthermore, these results indicate that ER restricted Bcl2 is capable of antagonizing not only apoptosis, but also a non-apoptotic, Bax/Bak independent, paraptosis-like form of cell death.

1. Introduction

Bap31, an endoplasmic reticulum (ER) localized polytopic transmembrane (TM) protein, plays a variety of roles in trafficking and quality control within the secretory system. Bap31 has been shown to function in ER retention/retrieval, cell surface export, survival/stabilization and ER associated degradation (ERAD) of select TM proteins [1–11]. Consistent with these disparate effects on ER protein trafficking is our recent finding that Bap31 associates with the Sec61 preprotein translocon at the ER, interacts with nascent client proteins as they emerge from the translocon, and escorts client proteins to ER complexes which determine their subsequent fate [9].

In addition to its role in protein trafficking, Bap31 also provides resistance to cytoplasmic events associated with membrane fragmentation in response to select apoptotic stimuli [12–14]. A number of apoptotic pathways involve cleavage of Bap31 by caspase-8; an event which both abrogates its antiapoptotic function and generates a membrane-embedded proapoptotic fragment, p20Bap31, or p20 [1,12,15–26]. Of note, ectopic expression of p20 was shown to induce apoptosis even in the absence of endogenous Bap31 [15].

p20 can also exert dominant negative (DN) interference with the protein transport functions of full-length Bap31 [1,4,9]. The influence of Bap31 or p20 in a particular cellular background, however, is likely dependent on the cargo protein under study, the relative levels of Bap31/p20 interacting partners, and the cell death competence of the system.

We have previously shown that p20 provides a proapoptotic signal via mobilization of ER Ca^{2+} stores. Ca^{2+} released from the ER is subsequently taken up by the mitochondria, leading to organelle fission. This alteration in mitochondrial morphology, which is likely accompanied by cristae remodeling, is thought to act as a "sensitizing signal" for release of the proapoptotic factor cytochrome c, allowing efficient mobilization of this molecule following mitochondrial outer membrane permeabilization (MOMP) [15,27]. Under physiological conditions, where apoptosis typically involves the induction of multiple pro-death proteins, Bap31 cleavage likely functions primarily as an amplification or sensitization signal, with another (mitochondrial) signal being directly responsible for MOMP. Nevertheless, prolonged ectopic expression of p20 does eventually lead to cell death [15].

Apoptosis associated with mitochondrial release of cytochrome c is, in most cases, regulated by the Bcl2 family of proteins [28]. The Bcl2 family consists of both pro- and anti-apoptotic members, where the proapoptotic multidomain Bcl2 proteins (Bax/Bak), act to permeabilize the outer mitochondrial membrane, leading to release of intermembrane proapoptotic factors, including cytochrome c. The antiapoptotic Bcl2 proteins act, both directly and indirectly, to inhibit Bax/Bak. The proapoptotic "BH3-only" Bcl2 proteins either inhibit the

* Corresponding author at: Department of Biochemistry, McIntyre Medical Sciences Building, Room 915D, McGill University, Montréal QC Canada, H3G 1Y6. Tel.: +1 514 398 7282; fax: +1 514 398 7384.
E-mail addresses: hannah.heath-engel@mail.mcgill.ca (H.M. Heath-Engel), bing.wang1@mcgill.ca (B. Wang), gordon.shore@mcgill.ca (G.C. Shore).

0167-4889/$ – see front matter © 2011 Elsevier B.V. All rights reserved.
doi:10.1016/j.bbamcr.2011.11.020

antiapoptotic family members, or activate Bax/Bak [29,30]. Although Bcl2 family members have been best studied with respect to their role at the mitochondria, they are also present at the ER, where they act, at least in part, to regulate ER Ca^{2+} stores and/or signaling [31–33].

Induction of Ca^{2+} release from the ER and ensuing apoptosis following p20 expression is likely regulated by Bcl2 proteins, as cell death was preceded by Bax activation, and could be inhibited by overexpression of either wild-type or ER-restricted Bcl2 (Bcl2b5) [15]. Additional support for the potential involvement of Bcl2 proteins in this pathway was provided by our study of the ER localized BH3-only protein Bik. Bik initiates a pathway similar to that seen for p20, and, in this system, both ER Ca^{2+} release and downstream mitochondrial events were shown to involve Bax/Bak, and could be inhibited by either Bcl2 or Bcl2b5 [34,35].

In our attempts to further explore the roles of Bax and Bak in the p20-induced cell death pathway, we used wild type (WT) and *Bax*/*Bak* double knockout (DKO) baby mouse kidney (BMK) immortalized epithelial cell lines, transformed by E1A and DN p53 [36]. We found, unexpectedly, that expression of p20 led to initiation of a non-apoptotic, paraptosis-like cell death pathway, in both WT and *Bax*/*Bak* DKO BMK cells. This p20-initiated pathway was characterized by an early rise, as opposed to release, of ER Ca^{2+} stores, as well as an early and dramatic dilation of the ER/nuclear envelope (NE). Thus the response to p20 expression can be dramatically different, dependent on cellular context.

Of particular importance, both p20-initiated cell death and ER dilation could be significantly delayed by overexpression of Bcl2b5 in the *Bax*/*Bak* DKO BMK cells. Bcl2 has been previously shown to function in a prosurvival capacity through inhibition of Bax/Bak, and our findings therefore represent evidence of a novel, Bax/Bak independent, prosurvival role for this protein at the ER.

2. Materials and methods

2.1. Cell lines and culture conditions

E1A/DNp53-transformed WT and *Bax*/*Bak* DKO BMK cells were kindly provided by Dr. Eileen White, Rutgers University, New Brunswick, NJ [36]. Cells were cultured at 37 °C in a humidified 5% CO_2 atmosphere, in RPMI 1640 media (Gibco) supplemented with 10% heat-inactivated FBS, 10 mM HEPES and 1 mM NaPyruvate. Cells stably expressing HA-Bcl2b5 in pcDNA3.1/Hygro(−) (Invitrogen) were maintained in media supplemented with 0.4 mg/ml hygromycin B (Invitrogen).

2.2. Constructs and gene expression

HA-p20, Flag-Bap31, Flag-crBap31, HA-A4, HA-Bik and HA-Bcl2b5 constructs were all expressed in either pcDNA3.0 or pcDNA3.1 (Invitrogen), and have been previously described [12,13,15,37,38]. Adenoviral expression vectors for HA-p20 (AdHA-p20), HA-Bik (AdHA-Bik) and rtTa (AdrtTa) have also been previously described [15,37]. Bcl2b5 refers to Bcl2 with the C-terminal membrane-targeting domain (aa 215–239) replaced with that of cytochrome b5 (aa 107–134). HA-Bcl2b5 was cloned into pcDNA3.1/Hygro(−) (Invitrogen), and DKO cells stably expressing HA-Bcl2b5 were obtained through transfection using Lipofectamine Plus (Invitrogen), followed by selection of individual clones with hygromycin B. As previously reported [39], Bcl2b5 was expressed at the ER, and not at the mitochondria, as determined by immunofluorescence microscopy (data not shown).

Adenoviral infection was carried out as previously described, on subconfluent cells, at the indicated MOI (multiplicity of infection, or plaque-forming units (pfu)/cell) [15,37,38]. All transient transfections were carried out using Lipofectamine 2000 (Invitrogen), as per manufacturer's instructions.

2.3. Measurement of cell death, caspase activity and ER Ca^{2+} stores

Cells were infected with the stated adenoviral expression constructs, and both adherent and floating cells were collected at the indicated times after infection. Cell death was determined through FACS analysis of propidium iodide (PI) uptake. Cells were washed once with PBS, and resuspended in PBS supplemented with 10 mg/ml propidium iodide (PI). Uptake of PI was determined by analysis with a Becton Dickinson FACScan Flow Cytometer. Samples were gated based on forward and side scatter, and the percentage of PI positive cells was determined based on intensity of fluorescence detected in the FL2 channel. Where indicated, infections were performed in the presence of ABT-737 (1 μM, GeminX) or zVAD-fmk (10 μM, MP Biomedicals). Caspase-3/7 activity was determined by measurement of DEVDase activity in 25 μg of cell lysate, as per manufacturer's instructions (Upstate Biotechnology). Thapsigargin (TG) releasable ER Ca^{2+} stores were determined using Fura2-AM (Molecular Probes), as previously described [15,34].

2.4. Immunofluorescence

Cells were seeded on glass coverslips and, where indicated, infected with AdHA-p20 or transfected with HA-p20, HA-A4, Flag-Bap31 or Flag-crBap31 expression vectors. Following fixation in 4% paraformaldehyde (PFA, Polysciences Inc), permeabilization and double label immunofluorescence staining were conducted as previously described [15]. Coverslips were mounted using ProLong Gold Antifade Reagent (Invitrogen), and images obtained using a Zeiss Axiovert 200 Inverted Microscope. Primary antibodies used were: mouse anti-HA (Babco), mouse anti-Flag M2 (Sigma), goat anti-lactate dehydrogenase (LDH, Chemicon), and polyclonal rabbit anti-calnexin (kindly provided by Dr. J. Bergeron, McGill University, Montreal, QC). Secondary antibodies used were: Alexa Fluor 488 or 594 conjugated goat anti-rabbit, goat anti-mouse, or rabbit anti-goat (Molecular Probes).

2.5. Light and electron microscopy

Phase contrast images were acquired using a Zeiss Axiovert 25 light-microscope, in combination with a Sony Cybershot DSC-S75 camera. For EM analysis, cells were grown in 10 cm^2 tissue culture dishes, trypsinized, fixed, and analyzed as previously described [34]. In all cases both adherent and floating cells were collected. For quantification of ER vacuolization, the percentage cellular area occupied by vacuolated ER/NE was determined using ImageJ [40]. A minimum of 50 cells was analyzed per condition.

2.6. Immunoprecipitation and Western blotting

For immunoprecipitation (IP) analysis, cells were infected with adenoviral vector encoding the stated construct, for the indicated times. Cells were solubilized at 4 °C in IP buffer (0.1% Triton X-100, 0.5% NP40, 50 mM HEPES-KOH, 150 mM NaCl, 1 mM EDTA pH7.5), and the lysate was cleared by centrifugation for 10 min at 13000 ×*g*. Lysates were incubated overnight at 4 °C with 2 μl of either hamster anti-humanBcl2 (anti-hBcl2) antibody (BD Pharmingen), or normal hamster serum (NHS) as a negative control. 10 μl of protein G-Sepharose (Amersham Biosciences) was added to the samples, and they were incubated at 4 °C for an additional 2 h. The beads were washed and then analyzed by Western blot using an anti-HA antibody, for detection of HA-p20, HA-Bik and HA-Bcl2b5. Lysis and IPs were done in the presence of protease inhibitors (1 μg/ml each of leupeptin, aproptinin and pepstatin, and 1 μM PMSF).

Western blotting was carried out by protein separation through SDS-PAGE, followed by transfer to nitrocellulose membrane and detection with specific antibodies. Blots were incubated with horseradish peroxidase (HRP)-conjugated secondary antibodies and visualized by enhanced chemiluminescence (Amersham). Primary antibodies used for Western blots were: mouse anti-HA, mouse anti-tubulin (Sigma), and mouse anti-actin (ICN Biomedicals).

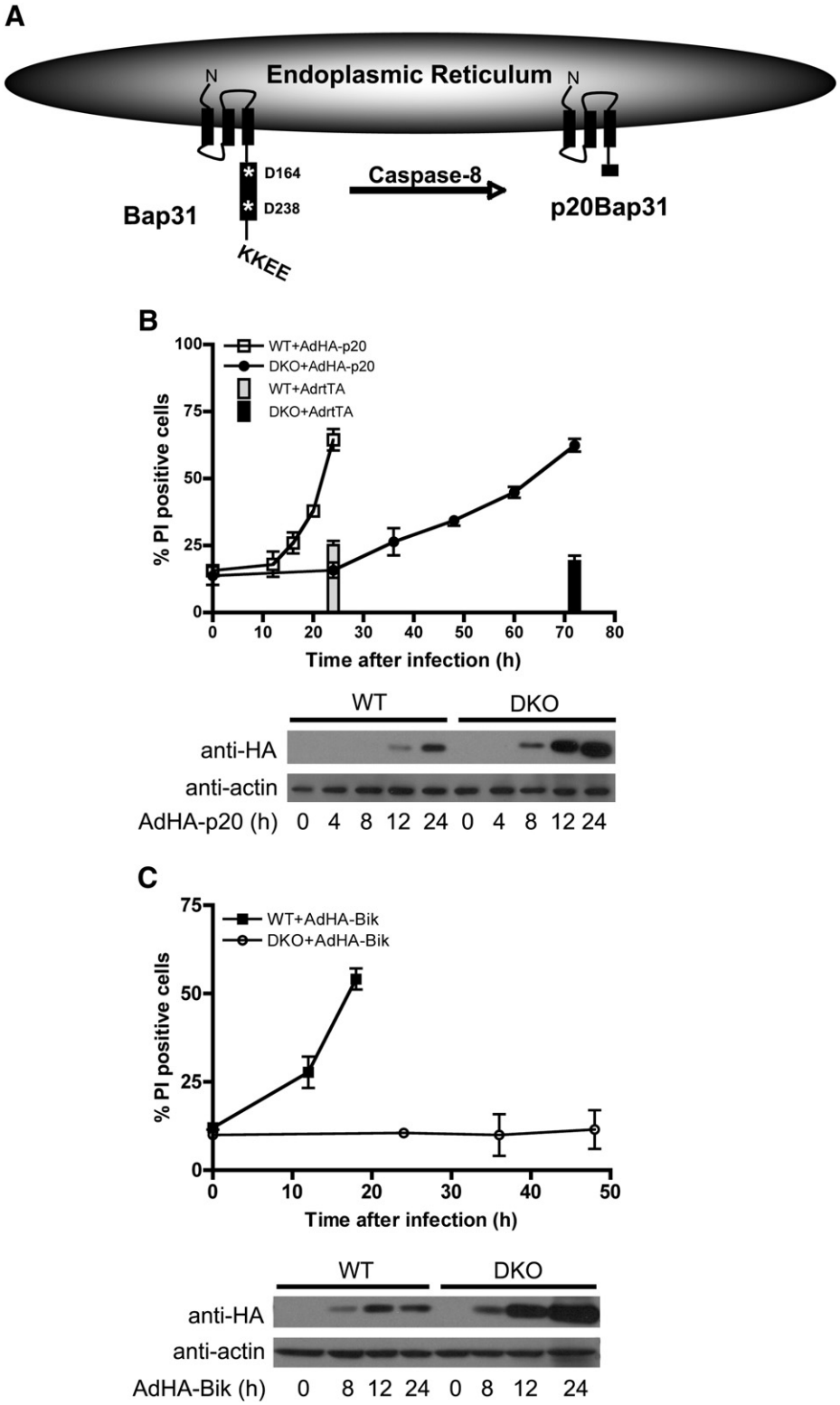

Fig. 1. Expression of p20, but not of Bik, leads to cell death even in the absence of Bax and Bak. (A) Schematic representation of Bap31 and p20 domains and topology at the ER. Caspase cleavage sites are indicated by asterisks. (B) p20 initiates cell death in both WT and DKO cells, although with delayed kinetics in the DKO cells. Cells were infected with either AdHA-p20 or AdrtTa (control), at an MOI of 80, for the indicated times, and cell death was determined by FACS analysis of PI uptake. Results are presented as the percentage of PI positive cells ($n = 3$, mean $\pm$ SD). (C) Bik expression leads to cell death in WT but not DKO cells. As in B, but cells were infected with AdHA-Bik instead of AdHA-p20. Expression of HA-p20 (B) and HA-Bik (C) at the indicated times was determined by Western blot with an anti-HA antibody, and is shown below the corresponding graph. Actin was used as a loading control.

3. Results

3.1. Ectopic expression of p20 leads to cell death even in the absence of Bax/Bak

Bap31 is a 246 amino acid ER localized protein with three predicted TM domains, a luminal N-terminal (N-T) domain, and a coiled-coil cytosolic C-terminal (C-T) domain (Fig. 1a). The C-T domain terminates with a canonical ER retrieval motif (KKEE). This motif, however, does not seem to be required for ER localization, as a truncated form of Bap31, lacking the KKEE motif, remains localized to the ER [1]. The C-T region of Bap31 also contains a variant death effector domain (vDED) flanked by two caspase 8/1 recognition sites, at aspartate 164 and 238. Although mouse Bap31 lacks the distal caspase recognition site, the protein is highly conserved, with 95% sequence identity between human and mouse [38]. Caspase cleavage at asp164 generates the p20 fragment in both mouse and human (Fig. 1a).

A number of apoptotic stimuli generate the proapoptotic p20 fragment, and we have previously shown, using a variety of human and murine cell lines, that ectopic expression of p20 triggers a proapoptotic pathway initiated by rapid depletion of ER Ca^{2+} stores [15]. We have also shown that the ER localized BH3-only protein Bik initiates a similar pathway, in which early ER Ca^{2+} release is dependent on Bax/Bak [34,35]. In order to determine the role of Bax/Bak in the p20-initiated pathway, we used WT and *Bax/Bak* DKO BMK cells, immortalized through transformation with E1A and DN p53 (hereafter referred to as WT and DKO cells). Using an adenoviral delivery system, we found that HA-tagged p20 (HA-p20) induces cell death, as measured by PI uptake, in both WT and DKO cells, although with delayed kinetics in the DKO cells (Fig. 1b). As expected based on previous studies [35], Bik mediated cell death was completely inhibited in the absence of Bax/Bak (Fig. 1c). As a negative control, WT and DKO cells were infected with adenovirus expressing the protein rtTa (Fig. 1b). No significant cell death was seen in the negative control, at up to 72 h post-infection for DKO cells, and at up to 24 h post-infection for WT cells. Expression levels of HA-p20 and HA-Bik in both WT and DKO cells are shown in Fig. 1b, c. Note that higher levels of both p20 and Bik can be tolerated in the absence of Bax/Bak.

3.2. Characterization of a novel, Bax/Bak independent, p20-initiated cell death pathway

The ability of HA-p20 (but not HA-Bik) to kill cells even in the absence of Bax/Bak points to an important difference between the p20 and Bik initiated pathways, and to a novel, Bax/Bak independent, p20-initiated mode of cell death. In order to further characterize this novel p20-initiated pathway, we looked at caspase activity and ER Ca^{2+} levels; cell death in response to either p20 or Bik was previously reported to involve both caspase activation and an early release of ER Ca^{2+} stores [15,34,35,37]. Surprisingly, although caspase activity was observed in both WT and DKO cells, incubation with the broad-spectrum caspase inhibitor zVAD-fmk did not significantly delay death in either cell line (Fig. 2a,b). Effective inhibition of executioner caspases-3 and 7 by zVAD-fmk was verified using a DEVDase activity assay (data not shown). Furthermore, p20 did not lead to the expected early release of ER Ca^{2+} stores, but rather to an initial rise in ER Ca^{2+}, followed by slow release, again in both WT and DKO cells (Fig. 2c). These results indicate that p20 can initiate more than one type of cell death. The first, previously characterized, type of cell death is dependent on both early release of ER Ca^{2+} and on caspase activity. The second type of cell death, described here, is independent of caspase activity, and involves an early rise in ER Ca^{2+} stores.

As the p20-induced pathway seen in this system appeared distinct from that previously described, we attempted to determine the early, or initiating, events. In this context, we found that the earliest

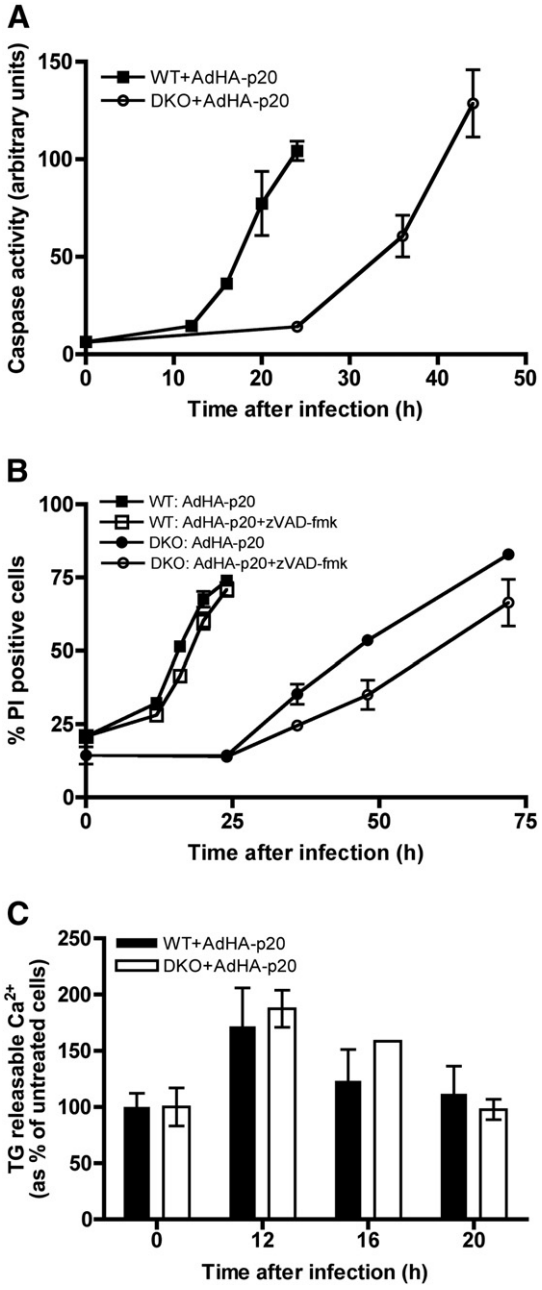

Fig. 2. Characterization of p20-initiated cell death in WT and DKO BMK cells. (A) p20 leads to caspase activation in both WT and DKO cells, although with delayed kinetics in the DKO cells. Cells were infected with AdHA-p20 for the indicated times, and effector caspase activity was determined by the ability of cell lysates to hydrolyze the fluorogenic caspase substrate DEVD-amc (n = 3, mean ± SD). (B) Caspase inhibition only slightly delays cell death, in both WT and DKO cells. Cells were infected with AdHA-p20 for the indicated times, in the presence or absence of zVAD-fmk. Viability was determined by FACS analysis of PI uptake, and results are presented as the percentage of PI positive cells (n = 3, mean ± SD). (C) ER Ca^{2+} levels show an initial increase, followed by delayed depletion, in both WT and DKO cells. Cells were infected with AdHA-p20 for the indicated times, loaded with Fura2-AM in Ca^{2+}-free buffer, and ER Ca^{2+} stores were determined based on the increase in Fura2 fluorescence following the addition of TG (n = 3, mean ± SD).

observable effect of p20 was a dramatic cytosolic vacuolization, which occurred soon after p20 expression, in both WT and DKO cells (Fig. 3a, b). Vacuolization appeared to result from extensive remodeling of the ER, as shown by immunofluorescent visualization using the ER marker calnexin (Fig. 3c). p20 was localized to the ER (as expected based on previous reports [15]), and both remodeling and "clumping" of the ER could be detected through visualization of

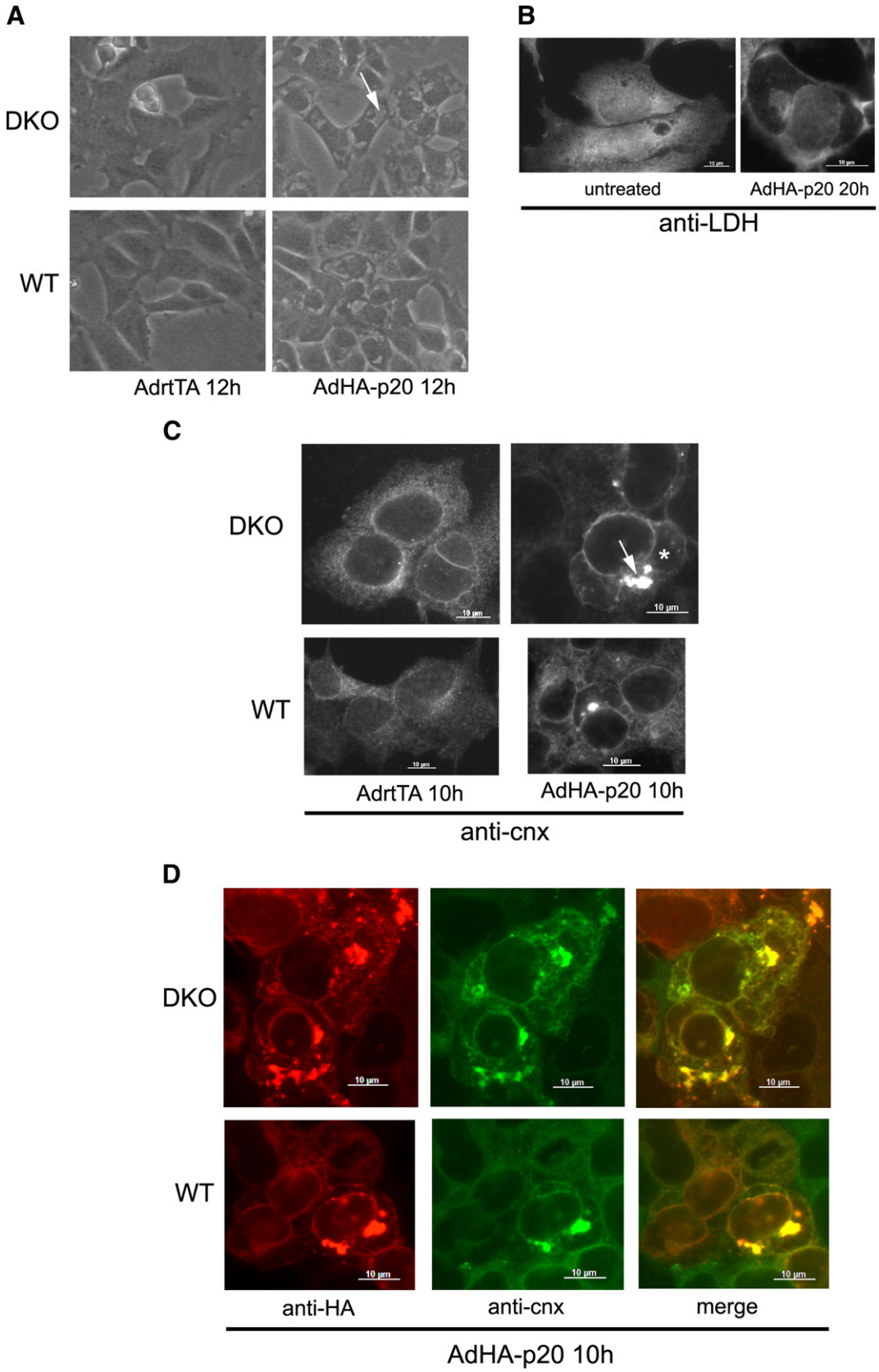

Fig. 3. Early p20-initiated changes in cell morphology. (A) Phase contrast images of early p20-initiated morphological changes. DKO (upper) and WT (lower) cells were infected with AdrtTa (control, left panels) or AdHA-p20 (right panels) for 12 h. The arrow indicates vacuolization in a p20-expressing cell. (B) Immunofluorescent visualization of p20-initiated cytosolic vacuolization in DKO cells. Cells were either left untreated, or infected with Ad-HAp20 for 20 h, and cytosol was visualized using an anti-LDH antibody. (C) Immunofluorescent visualization of p20-initiated changes in ER morphology. DKO (upper) and WT (lower) cells were infected with AdrtTa (control, left panels) or AdHA-p20 (right panels) for 10 h, and ER was visualized using an antibody to the integral ER membrane protein calnexin (cnx). Areas of both ER vacuolization (star) and aggregation (arrow) can be seen in p20 expressing cells. (D) ER localization of HA-p20. DKO (upper) and WT (lower) cells were infected with AdHA-p20 for 10 h. HA-p20 was visualized via staining with an anti-HA antibody, and calnexin was used as an ER marker. HA-p20 is shown in the left panel, cnx is shown in the center panel, and an overlay of the left and center panels is shown in the right panel. All infections were done at an MOI of 40.

HA-p20 with an anti-HA antibody (Fig. 3d). The effect of p20 expression on organelle morphology was also examined using electron microscopy (Fig. 4). Electron micrographs of AdHA-p20 infected cells showed progressive dilation of the ER and NE, ultimately leading to dramatic cellular vacuolization, in both DKO (Fig. 4a) and WT (not shown) cells. Mitochondria appeared either normal, condensed or swollen, but did not show the cristae remodeling characteristic of Bik-initiated ER Ca^{2+} transmission to this organelle [34]. Both WT and DKO cells yielded evidence of necrosis in response to p20, with observations of organelle swelling and plasma membrane rupture, in the absence of typical apoptotic morphology (chromatin condensation, cell shrinkage, blebbing) (Fig. 4a). In some cases there was also evidence of amplified, organized smooth ER (OSER), which seemed to be generated within vacuolated ER/NE (Fig. 4b). OSER arises due to overexpression of dimerization competent ER membrane proteins, and can be seen as bright spots (i.e. "clumping") in immunofluorescent images (Fig. 3c, d) [41].

3.3. Effect of ER-restricted Bcl2 on p20-initiated events in DKO cells

Based on the previously reported ability of both WT and ER-restricted Bcl2 to inhibit p20-initiated apoptosis [15], as well as the fact that Bcl2 can also, in some cases, inhibit non-apoptotic cell death [42–51], we chose to examine the effect of ER-restricted Bcl2 on the p20-initiated pathway in DKO cells. In order to do this, we generated DKO cells stably expressing an HA-tagged, ER-restricted form

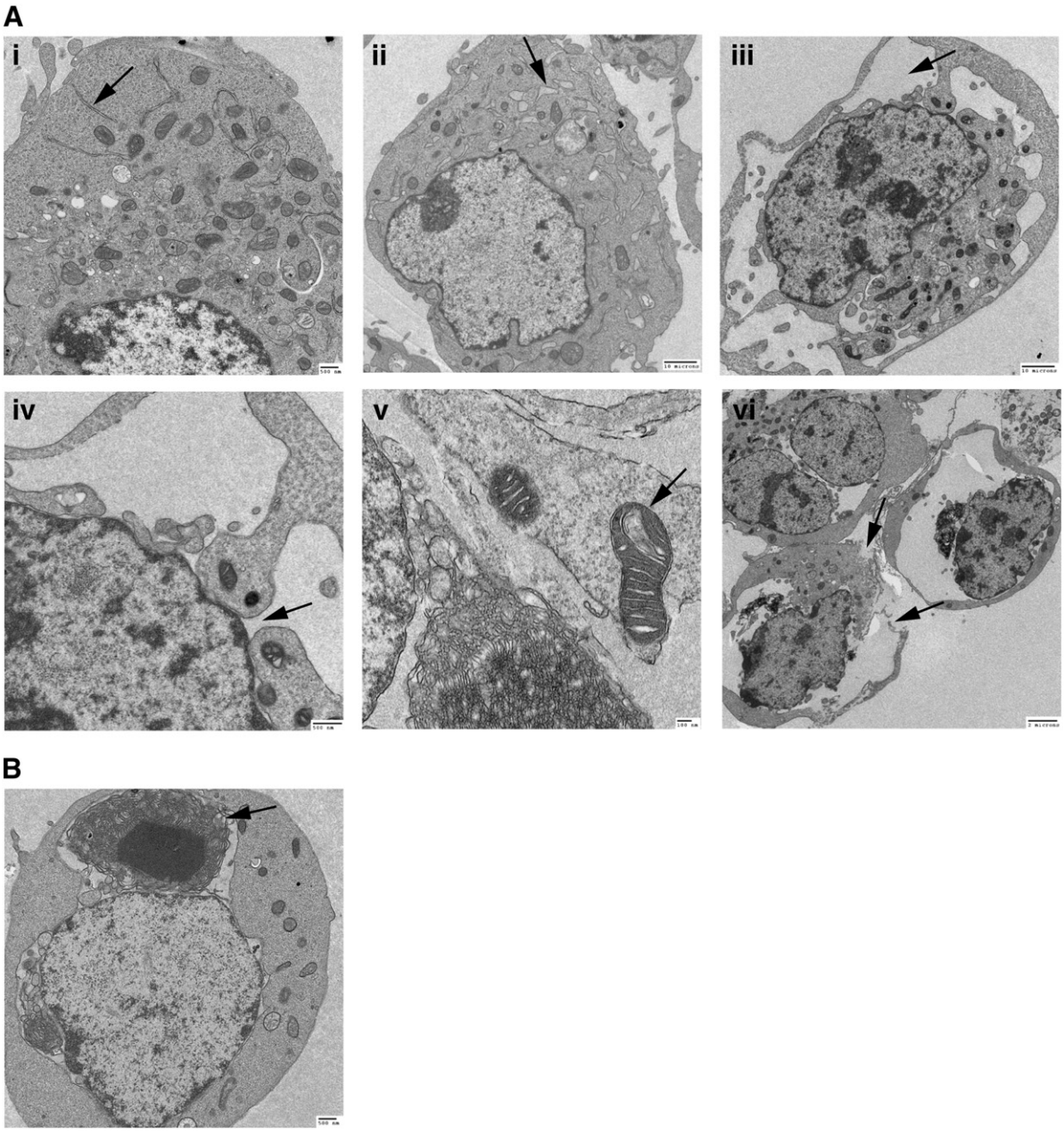

Fig. 4. Early p20-initiated changes in cell morphology visualized by electron microscopy. (A) Representative images of the phenotypic effects of p20 expression on E1A/DNp53 transformed BMK cells. DKO cells were either untreated (i) or infected with AdHA-p20 at an MOI of 40 (ii–vi). (i) An untreated DKO cell with normal ER (arrow). (ii) Modest expansion of the ER in an AdHA-p20 infected DKO cell. Although swollen, the reticular structure of the ER is still visible (arrow). (iii) Extensive swelling/remodeling of the ER/NE in an AdHA-p20 infected cell. (iv) Higher magnification of the cell in (iii) showing a dilated nuclear pore. (v) Apparently normal mitochondrial ultrastructure (arrow), in the presence of extensive ER remodeling. (vi) Apparent necrosis of an AdHA-p20 infected cell involving plasma membrane rupture (arrows). Note the lack of chromatin condensation, and normal or swollen appearance of mitochondria, as well as the dramatic vacuolization of the ER/NE. (B) p20-induced formation of organized smooth ER (OSER, arrow) in a DKO BMK cell, following infection with AdHA-p20 for 12 h, at an MOI = 80.

of Bcl2, HA-Bcl2b5 [15,39] (DKO/HA-Bcl2b5 cells). Surprisingly, Bcl2b5 was able to delay both p20-associated cell death and ER/NE vacuolization in the DKO cells (Fig. 5). It should be noted, however, that the protective effects of Bcl2b5 were ultimately overwhelmed in the face of increasing expression levels of p20 (Fig. 5a). The effect of Bcl2b5 on p20-initiated ER dilation could be seen using both light

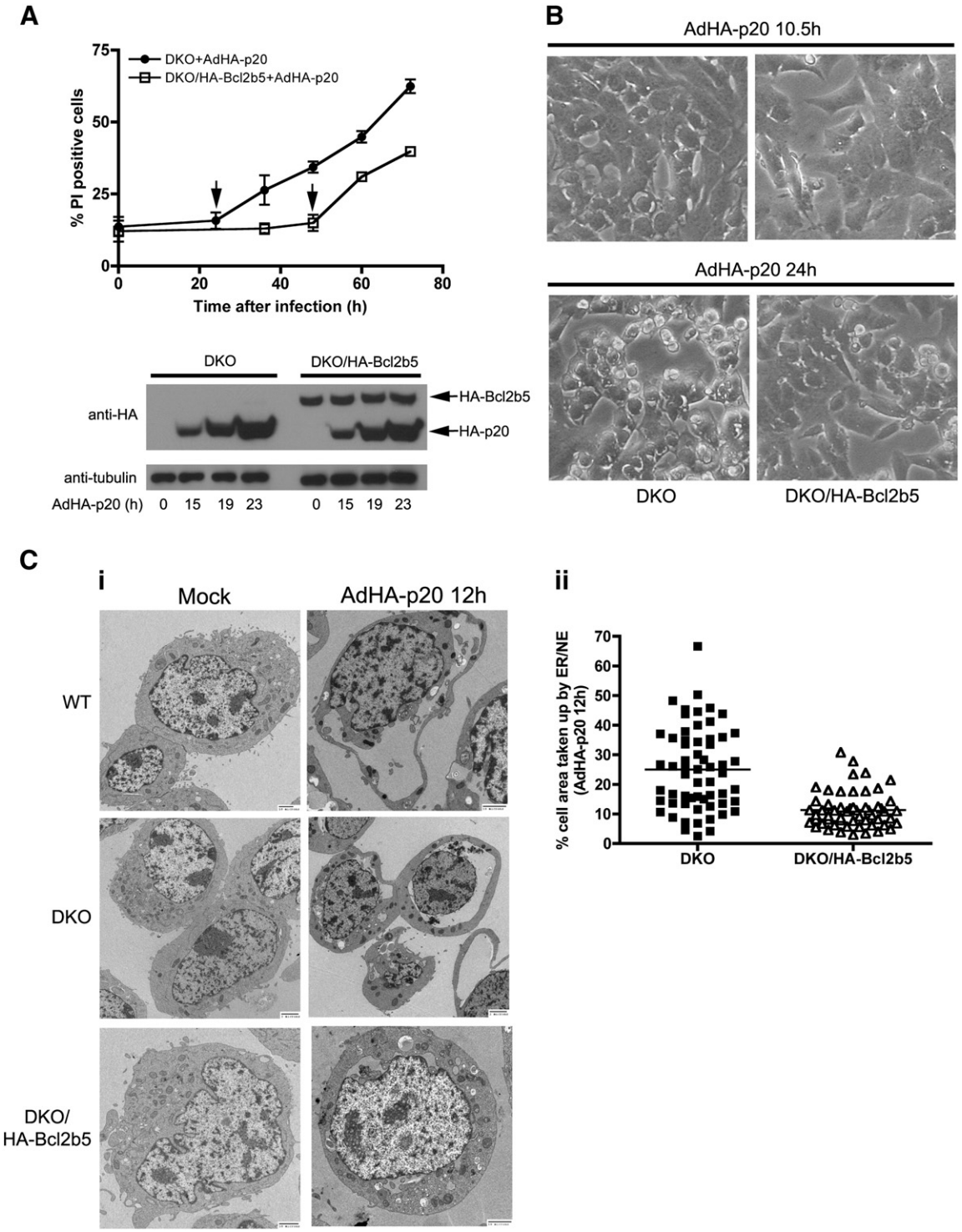

Fig. 5. ER-restricted Bcl2 delays both cell death and ER remodeling in the absence of Bax/Bak. (A) ER-restricted Bcl2 (Bcl2b5) delays p20-initiated cell death in DKO cells. DKO or DKO/HA-Bcl2b5 cells were infected with AdHA-p20, at an MOI of 80, for the indicated times, and viability was determined by FACS analysis of PI uptake. Results are presented as the percentage of PI positive cells ($n = 3$, mean ± SD). Note that DKO cells began to die between 24 and 36 h after infection with AdHA-p20, while no cell death was observed in DKO/HA-Bcl2b5 cells until at least 48 h after infection (arrows). Expression of HA-p20 in either DKO or DKO/HA-Bcl2b5 cells at the indicated times was determined by Western blot with an anti-HA antibody, as shown in the lower panel. Tubulin was used as a loading control. (B) Bcl2b5 delays p20-initiated vacuolization and detachment of DKO cells. DKO (left) and DKO/HA-Bcl2b5 (right) cells were infected with AdHA-p20 (MOI = 40), and representative images were acquired at 10.5 h (upper panels) and 24 h (lower panels) after infection. Note the decreased level of vacuolization in DKO/HA-Bcl2b5 cells at 10.5 h, and the lower level of both vacuolization and detachment at 24 h. (C) Electron microscopic visualization of the effect of Bcl2b5 on p20-initiated ER expansion in DKO cells. (i) Representative pictures of untreated (left column) and AdHA-p20 infected (right column) WT, DKO, and DKO/HA-Bcl2b5 cells. (ii) Quantification of ER remodeling in DKO and DKO/HA-Bcl2b5 cells, via determination of the percentage of cellular area taken up by vacuolated ER. Infection was for 12 h, at an MOI = 40.

microscopy (Fig. 5b) and EM (Fig. 5c). Results from an EM experiment were quantified via determination of percentage cellular area occupied by vacuolated ER/NE (Fig. 5c).

A direct interaction between Bcl2 and p20 was previously reported [38] and the established cytoprotective role of Bcl2 depends on binding and sequestration of proapoptotic proteins [30,52,53]. A potential interaction between Bcl2b5 and p20 in the DKO cells was therefore investigated using co-immunoprecipitation, and the role of the Bcl2b5 BH3 binding pocket was addressed using the small molecule BH3 mimetic ABT-737 [54,55]. If the protective effect of Bcl2b5 required the Bcl2 binding pocket, ABT-737 would be expected to provide a sensitizing effect. We choose to look at the effect of ABT-737 on cell death in DKO/HA-Bcl2b5 cells at 48 h after infection with AdHA-p20; a time at which a significant proportion of DKO, but not DKO/HA-Bcl2b5 cells, were PI positive (Fig. 5a). Using the above-described techniques we found that, in the DKO/HA-Bcl2b5 cells, no interaction could be detected between HA-p20 and HA-Bcl2b5 (Fig. 6a), and, in addition, that ABT-737 was unable to overcome the protective effect of Bcl2b5 with respect to p20 (Fig. 6b). In these E1A/DNp53 transformed BMK cells, Bcl2b5 therefore provides a Bax/Bak independent protective effect, which, based on the results presented in Fig. 6, is likely independent of direct interaction with p20, and of the BH3 binding pocket.

One function of Bcl2 that does not depend on either the BH3 binding pocket or on Bax/Bak is that of regulation of ER Ca^{2+} stores [56,57]. As p20-initiated death in both WT and DKO cells was characterized by an early rise in ER Ca^{2+} stores, and Bcl2 has been reported to lower ER Ca^{2+} content [15,58–60], we hypothesized that the protective effect of Bcl2b5 could be due to decreased ER Ca^{2+}, and, furthermore, that intact ER Ca^{2+} stores might be required for p20-induced ER/NE dilation. Consistent with this hypothesis, we found that ER Ca^{2+} stores were in fact lower in DKO/HA-Bcl2b5 cells than in DKO cells (Fig. 7a). In addition, we found that depletion of ER Ca^{2+} stores with a low concentration of thapsigargin (TG) prior to expression of p20 significantly decreased the number of cells with remodeled ER (Fig. 7b). These results indicate that intact ER Ca^{2+} stores are likely required for p20-mediated disruption of ER structure, and that the protective effect of Bcl2b5 may be due to modulation of ER Ca^{2+}.

3.4. ER remodeling can be initiated by overexpression of full-length Bap31, but not of other ER TM proteins

The ER/NE vacuolization seen in response to p20 is highly reminiscent of that seen in certain forms of ER stress [61–74], and p20 has been reported to interfere with protein trafficking in several systems, likely through a dominant negative effect on full-length Bap31 [1,4,9]. If dysregulation of Bap31-mediated protein trafficking underlies cell death in this system, then a similar effect might be seen following overexpression of the full-length protein. This was in fact the case, as overexpression of Bap31 also resulted in ER remodeling. This was not due to caspase cleavage of the full-length protein following expression, as a caspase-resistant form of Bap31 (crBap31) also led to disruption of ER structure (Fig. 8a). Bap31/p20 initiated ER dilation was not a nonspecific effect of overexpression of an ER TM protein, as normal morphology was maintained following overexpression of the polytopic ER TM protein A4 [75] (Fig. 8b). Both p20 and A4 were tagged with HA, and were overexpressed to comparable levels. Similar results to those shown for A4 were observed following overexpression of the ER TM proteins Derlin-1 and calnexin (not shown).

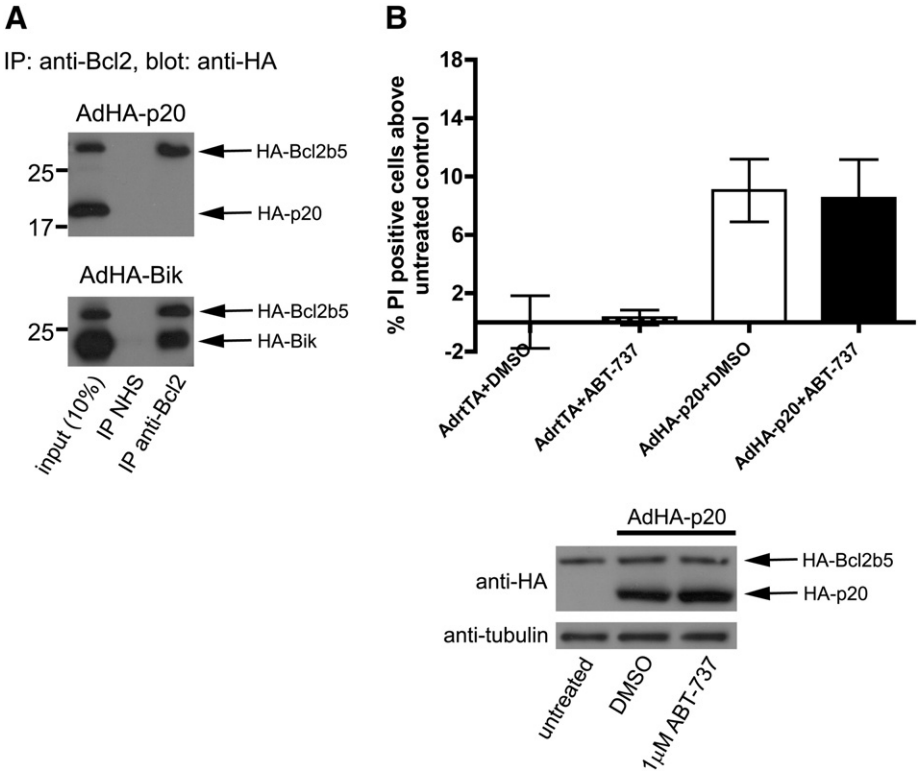

Fig. 6. The effect of Bcl2b5 on the p20-initiated pathway in DKO cells does not involve either a detectable interaction between the two proteins or the Bcl2b5 BH3 binding region. (A) There is no detectable interaction between HA-Bcl2b5 and HA-p20 in DKO cells. DKO/HA-Bcl2b5 cells were infected overnight with either AdHA-p20 (MOI = 40) or AdHA-Bik (positive control, MOI = 25). Cells were disrupted using IP buffer (0.1% Triton X-100, 0.5% NP40), and 800 μg of whole cell lysate was subjected to IP with either hamster anti-hBcl2 antibody, or NHS (control). 200 μg of each IP, along with 20 μg (10%) of input, was analyzed by Western blot with an anti-HA antibody, to detect HA-p20, HA-Bik, and HA-Bcl2b5. (B) The small molecule BH3 mimetic ABT-737 does not affect HA-p20 initiated death in DKO/HA-Bcl2b5 cells. DKO/HA-Bcl2b5 cells were infected with either AdHA-p20 (MOI = 80) or AdrtTA (control, MOI = 80), in the presence of either 1 μM ABT-737 or DMSO (vehicle), and viability was determined by FACS analysis of PI uptake 48 h after infection. Results are presented as the percentage of PI positive cells above that present in the negative (untreated) control (n = 3, mean ± SD). Expression of HA-p20, in the presence or absence of ABT-737, was determined by Western blot with an anti-HA antibody, following a 12 infection with AdHA-p20 at an MOI of 80. Tubulin was used as a loading control.

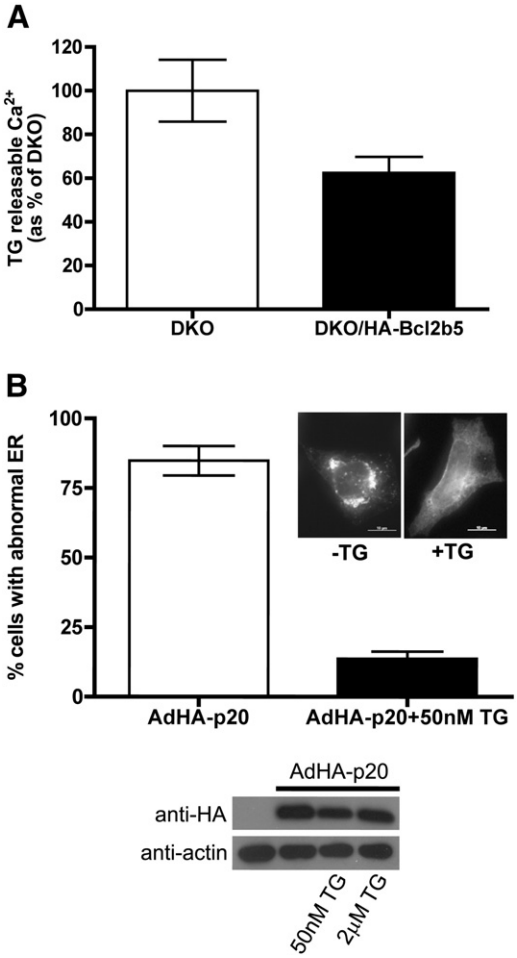

Fig. 7. Bcl2b5 lowers ER Ca^{2+} stores in DKO cells, and intact ER Ca^{2+} stores are required for p20-initiated ER remodeling. (A) ER Ca^{2+} stores are lower in DKO/HA-Bcl2b5 cells than in DKO cells. Cells were loaded with Fura2-AM in Ca^{2+}-free buffer, and ER Ca^{2+} stores were determined based on the increase in Fura2 fluorescence following the addition of TG (n = 3, mean ± SD). (B) Intact ER Ca^{2+} stores are required for p20-initiated ER remodeling. ER Ca^{2+} stores in DKO cells were depleted using a low (50 nM) concentration of TG prior to infection with AdHA-p20 (MOI = 40, 16 h), and ER structure was visualized through immunofluorescent detection of HA-p20 with an anti-HA antibody. The percentage of cells with remodeled ER was determined by visual inspection and quantification, and at least 200 cells per condition were examined for each experiment (n = 4, mean ± SD). Inset shows representative immunofluorescence images of HA-p20 expressing cells, with and without TG. The lower panel shows the expression level of HA-p20, in the presence and absence of TG, as determined by Western blot with an anti-HA antibody. Actin was used as a loading control.

4. Discussion

4.1. Identification of a novel p20 initiated, Bax/Bak independent, cell death pathway

Both p20 and the ER localized BH3-only protein Bik were previously shown to provide a sensitizing signal with respect to Bax/Bak associated mitochondrial apoptosis, dependent on an early release of ER Ca^{2+} stores and on ER–mitochondria Ca^{2+} transmission [15,34,35]. We have now uncovered a second p20-initiated pathway, wherein, in the absence of early ER Ca^{2+} release, p20 expression leads to non-apoptotic cell death, associated with dramatic dilation of the ER/NE. Of note, this second pathway was not initiated by ectopic expression of Bik, pointing to an important difference in the mode of action of these two proteins.

Cell death in this system, in spite of detectable caspase activity, could not be inhibited by zVAD-fmk (a broad spectrum caspase inhibitor). In addition, EM analysis of dying cells showed evidence of necrosis (organelle swelling and plasma membrane rupture), but not of apoptosis (nuclear condensation, cell shrinkage, blebbing), or of the mitochondrial cristae remodeling associated with Bik-initiated Ca^{2+} transmission [34]. The earliest observable effect of p20 expression, in both WT and *Bax*/*Bak* DKO BMK cells, was a dramatic vacuolization of the ER/NE, accompanied by a rise in ER Ca^{2+} stores. ER/NE dilation was apparently dependent on intact ER Ca^{2+} stores, as depletion of ER Ca^{2+} via pretreatment with a low concentration of TG significantly decreased the number of cells displaying ER/NE remodeling.

The above-described changes in ER/NE morphology are similar to those seen during paraptosis: a caspase-independent, non-apoptotic, form of programmed cell death culminating in necrosis [51,74,76–83]. Paraptosis, although poorly defined at the molecular level, is characterized by progressive organelle, primarily ER, vacuolization [76,82,84]. Of potential significance, a paraptosis-like form of cell death is often seen in response to ER stressors, in particular those involving both increased accumulation of misfolded proteins and inhibition of ERAD [61–65,67–74,81,85]. Although p20 has been shown to initiate early ER Ca^{2+} release and downstream mitochondrial alterations in several cell types [15], it has also been shown to interfere with protein trafficking, possibly via a dominant negative effect on full length Bap31 [1,4,9]. As Bap31 plays a role in both ERAD [9,10] and protein export from the ER [4,6,7], it is conceivable that disruption of Bap31 dependent protein trafficking (in this case through expression of p20) could lead to both increased protein load within the ER, and a block in degradation.

It therefore appears that in certain cell types or under certain conditions, p20 does not trigger ER Ca^{2+} release, but instead stimulates paraptosis-like cell death, possibly via ER stress. Why some cell types release ER Ca^{2+} in response to p20 while the E1A/DNp53 transformed cells used here do not, however, remains to be determined. The fact that the SERCA inhibitor thapsigargin readily stimulated release of ER Ca^{2+} stores in these BMK cells and indeed such release of ER Ca^{2+} protected against p20-induced ER changes (Fig. **7**) suggests that the Ca^{2+} release channel is functional, and that for reasons that remain to be elucidated p20 is incapable of coupling to such release, in contrast to KB and H1299 cells.

Whether or not the paraptosis-like cell death observed in this system stems from the influence of p20 on ER protein trafficking also remains to be determined. It is, however, noteworthy that over-expression of full length Bap31, but not of other integral ER proteins, also caused ER remodeling in the E1A/DNp53-transformed BMK cells. Moreover, the ER remodeling induced by over-expression of Bap31 or crBap31 was also associated with cell toxicity (data not shown).

Based on the above evidence, we propose that p20 can initiate two distinct pro-death pathways, dependent on the underlying physiology of the cell type under study (Fig. 9). The first of these, which was previously described [15], is proapoptotic, involves an early release of ER Ca^{2+} stores, and provides a sensitizing effect with respect to Bax/Bak dependent mitochondrial release of cytochrome c. The second pathway, described herein for the first time, is characterized by an initial rise, as opposed to release, of ER Ca^{2+} stores, and involves a dramatic dilation of the ER/NE. This pathway ultimately results in non-apoptotic cell death, potentially due to disruption of ER homeostasis. The early events in this pathway, including increased ER Ca^{2+} content and ER/NE dilation, are apparently independent of Bax/Bak; occurring at about the same time in both WT and DKO cells. The later events, including caspase activity and loss of membrane integrity, can be delayed, but not completely inhibited, by the loss of Bax/Bak. Bax/Bak therefore appear to accelerate execution, but not initiation, of this form of cell death.

It should be noted that Bax/Bak deficient cells were previously shown to display lowered ER Ca^{2+} stores [86]. Based on the apparent dependence of p20 initiated ER remodeling on intact ER Ca^{2+} stores, ER remodeling, in addition to ultimate cell death, should be delayed in the absence of Bax/Bak. Although onset of ER dilation appeared to occur at approximately the same time, and to the same extent, in

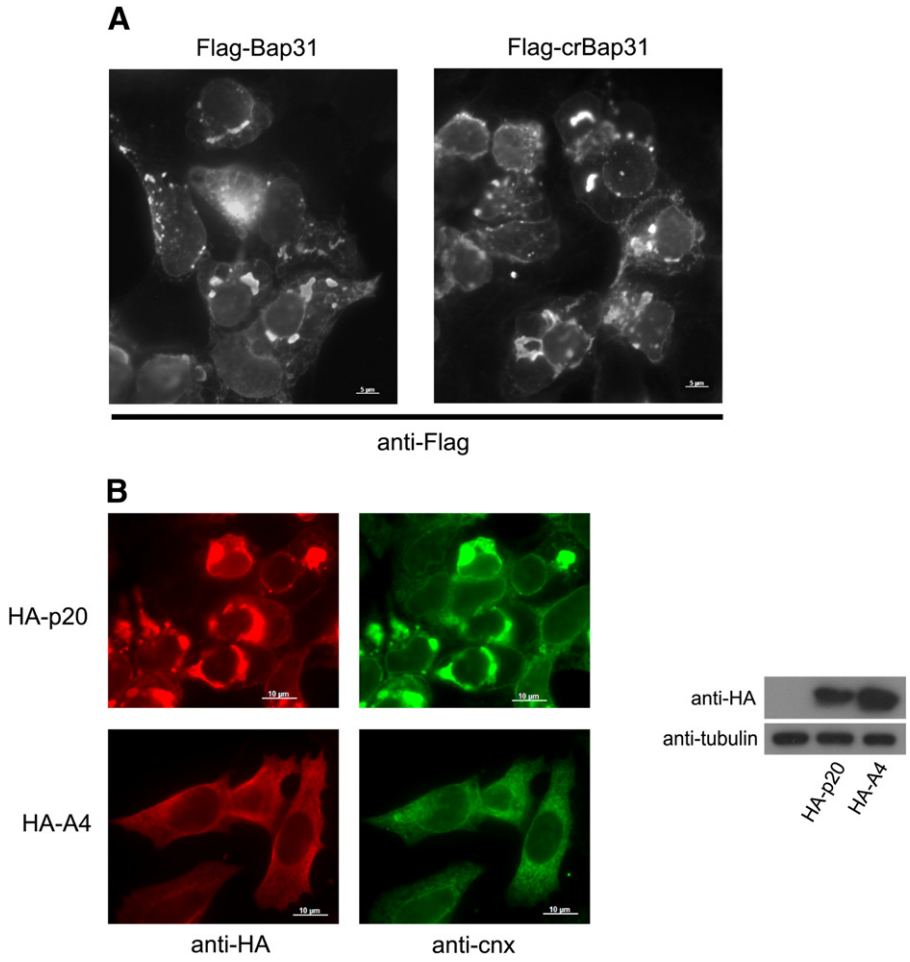

Fig. 8. Overexpression of full length Bap31, but not of the integral ER membrane protein A4, leads to ER remodeling in DKO cells. (A) Overexpression of either Bap31 or crBap31 results in ER remodeling. DKO cells were transiently transfected with either Flag-Bap31 or Flag-crBap31 for 20 h, and ER was visualized by staining with an anti-Flag antibody. (B) Overexpression of the polytopic ER TM protein A4 does not affect ER morphology. DKO cells were transiently transfected with either HA-p20 (upper panel) or HA-A4 (lower panel) for 11 h, and ER was visualized by staining with both an anti-HA antibody (left) and an anti-cnx antibody (right). Expression levels of HA-p20 and HA-A4 were determined by Western blot with an anti-HA antibody. Tubulin was used as a loading control.

both WT and DKO BMK cells (unpublished observations and Figs. 3 and 5), the precise timing of this event was not determined. It is therefore possible that the loss of Bax/Bak did in fact provide a slight delay in the onset of ER dilation. Alternatively, the reduction in ER Ca^{2+} stores as a result of Bax/Bak deletion may not have been sufficient to provide a protective effect in this system.

Another interesting feature of the p20 death pathway described here is that effector caspases were activated by p20, yet cell death was by a paraptosis-like mechanism, and pan-caspase inhibition by zVAD-fmk was without effect. Thus, there is an apparent block between effector caspase activation and the ability to execute apoptosis in a time frame that would precede the paraptosis response. In future studies it will be intriguing to determine if this is linked to the defect in Ca^{2+} release by p20. Caspase activation was a late event, occurring well after both ER dilation and the rise in ER Ca^{2+} stores, and at approximately the same time as loss of viability (Figs. 1–3). Furthermore, both loss of mitochondrial membrane potential and cytochrome c release (indicating loss of mitochondrial integrity) were seen at approximately the same time as capsase activity was first observed (data not shown). Caspase activation may therefore, in this case, be a consequence of generalized disruption of organelle structure, which, as a result of mitochondrial membrane permeabilization and/or rupture, would lead to cytochrome c dependent caspase activation, concurrent with necrotic cell death. In support of this hypothesis, there is a growing body of evidence indicating that multiple cell death pathways are often initiated in concert, and that caspase inhibition, in many cases, is not sufficient to inhibit ultimate cell death [84,87,88].

4.2. Effect of ER-restricted Bcl2 on the p20-initiated pathway in DKO BMK cells

Bcl2 can inhibit a variety of apoptotic pathways, and, in most cases, is thought to act through inhibition of Bax/Bak [29]. Bcl2 has also, however, been reported to inhibit non-apoptotic cell death [42–51], and can function independently of Bax/Bak, as shown with respect to its role in ER Ca^{2+} handling [56]. As both WT and ER-restricted Bcl2 were able to inhibit the proapoptotic p20-initiated pathway [15], we decided to investigate the effect of Bcl2b5 on non-apoptotic p20-associated cell death in DKO BMK cells. We found that Bcl2b5 was able to significantly delay both cell death and ER/NE vacuolization in the absence of Bax/Bak. This effect of Bcl2b5 did not appear to involve the BH3 binding pocket, and no interaction could be detected between Bcl2b5 and p20. Based on these observations, in combination with the observed decrease in ER Ca^{2+} stores in the presence of Bcl2b5, and the importance of intact ER Ca^{2+} stores in p20-initiated ER dilation, we propose that the protective effect of Bcl2b5 in this system is likely due to modulation of ER Ca^{2+} levels. Bcl2 is frequently overexpressed in various malignancies, and sensitization of tumor cells to apoptosis via Bcl2 inhibition using BH3 mimetics is currently a topic of active research [55]. Evidence for Bcl2

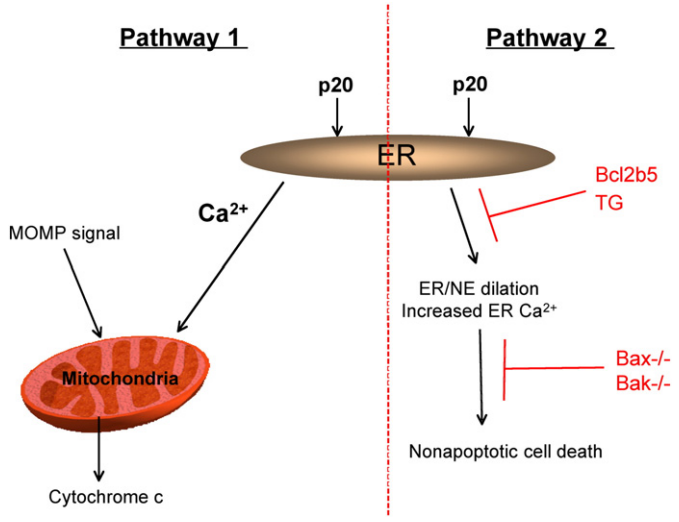

Fig. 9. Proposed model for p20 initiated cell death pathways. Pathway 1 refers to the previously described p20 initiated pathway, and Pathway 2 refers to the novel p20 initiated pathway described in this paper. See text for details.

mediated inhibition of non-apoptotic cell death, independent of both Bax/Bak and of the BH3 binding pocket, therefore has potentially important clinical implications.

In conclusion, we have identified a Bax/Bak independent paraptosis-like cell death pathway initiated by expression of p20 (Fig. 9). Early events in this pathway include a rise in ER Ca^{2+} stores, as well as dramatic dilation of the ER/NE. We propose that this pathway reflects p20/Bap31-mediated disruption of ER homeostasis in susceptible cell types. Of particular importance, both p20-initiated cell death and initial ER dilation could be significantly delayed by overexpression of ER-restricted Bcl2 in the DKO cells. This ability of ER localized Bcl2 to inhibit Bax/Bak independent non-apoptotic cell death may have important implications with respect to the design and implementation of therapeutic drugs.

Acknowledgements

The authors would like to thank Nhi Nguyen for generating the DKO/HA-Bcl2b5 cells, and Dr. Mai Nguyen for excellent technical assistance and helpful discussions. We are grateful to Dr. Heidi McBride and Peter Rippstein for the use of their EM facilities and for their technical assistance and expert opinion. We are also grateful to Ken McDonald, Dr. Claire Brown and Aleks Spurmanis for their technical assistance and guidance, and we thank Dr. Eileen White for providing the WT and DKO BMK cells. HMHE is the recipient of a Terry Fox Foundation Studentship, from the National Cancer Institute of Canada. This work was supported by research grants from the Canadian Institutes of Health Research and the National Cancer Institute of Canada.

References

[1] W.G. Annaert, B. Becker, U. Kistner, M. Reth, R. Jahn, Export of cellubrevin from the endoplasmic reticulum is controlled by BAP31, J. Cell Biol. 139 (1997) 1397–1410.
[2] E. Szczesna-Skorupa, B. Kemper, BAP31 is involved in the retention of cytochrome P450 2C2 in the endoplasmic reticulum, J. Biol. Chem. 281 (2006) 4142–4148.
[3] W.W. Schamel, S. Kuppig, B. Becker, K. Gimborn, H.P. Hauri, M. Reth, A high-molecular-weight complex of membrane proteins BAP29/BAP31 is involved in the retention of membrane-bound IgD in the endoplasmic reticulum, Proc. Natl. Acad. Sci. U.S.A. 100 (2003) 9861–9866.
[4] M. Stojanovic, M. Germain, M. Nguyen, G.C. Shore, BAP31 and its caspase cleavage product regulate cell surface expression of tetraspanins and integrin-mediated cell survival, J. Biol. Chem. 280 (2005) 30018–30024.
[5] M.E. Paquet, M. Cohen-Doyle, G.C. Shore, D.B. Williams, Bap29/31 influences the intracellular traffic of MHC class I molecules, J. Immunol. 172 (2004) 7548–7555.
[6] J.J. Ladasky, S. Boyle, M. Seth, H. Li, T. Pentcheva, F. Abe, S.J. Steinberg, M. Edidin, Bap31 enhances the endoplasmic reticulum export and quality control of human class I MHC molecules, J. Immunol. 177 (2006) 6172–6181.
[7] F. Abe, N. Van Prooyen, J.J. Ladasky, M. Edidin, Interaction of Bap31 and MHC class I molecules and their traffic out of the endoplasmic reticulum, J. Immunol. 182 (2009) 4776–4783.
[8] B. Wang, J. Pelletier, M.J. Massaad, A. Herscovics, G.C. Shore, The yeast split-ubiquitin membrane protein two-hybrid screen identifies BAP31 as a regulator of the turnover of endoplasmic reticulum-associated protein tyrosine phosphatase-like B, Mol. Cell. Biol. 24 (2004) 2767–2778.
[9] B. Wang, H. Heath-Engel, D. Zhang, N. Nguyen, D.Y. Thomas, J.W. Hanrahan, G.C. Shore, BAP31 interacts with Sec61 translocons and promotes retrotranslocation of CFTRDeltaF508 via the derlin-1 complex, Cell 133 (2008) 1080–1092.
[10] Y. Wakana, S. Takai, K. Nakajima, K. Tani, A. Yamamoto, P. Watson, D.J. Stephens, H.P. Hauri, M. Tagaya, Bap31 is an itinerant protein that moves between the peripheral endoplasmic reticulum (ER) and a juxtanuclear compartment related to ER-associated degradation, Mol. Biol. Cell 19 (2008) 1825–1836.
[11] G. Lambert, B. Becker, R. Schreiber, A. Boucherot, M. Reth, K. Kunzelmann, Control of cystic fibrosis transmembrane conductance regulator expression by BAP31, J. Biol. Chem. 276 (2001) 20340–20345.
[12] M. Nguyen, D.G. Breckenridge, A. Ducret, G.C. Shore, Caspase-resistant BAP31 inhibits fas-mediated apoptotic membrane fragmentation and release of cytochrome c from mitochondria, Mol. Cell. Biol. 20 (2000) 6731–6740.
[13] B. Wang, M. Nguyen, D.G. Breckenridge, M. Stojanovic, P.A. Clemons, S. Kuppig, G.C. Shore, Uncleaved BAP31 in association with A4 protein at the endoplasmic reticulum is an inhibitor of Fas-initiated release of cytochrome c from mitochondria, J. Biol. Chem. 278 (2003) 14461–14468.
[14] A. Ducret, M. Nguyen, D.G. Breckenridge, G.C. Shore, The resident endoplasmic reticulum protein, BAP31, associates with gamma-actin and myosin B heavy chain, Eur. J. Biochem. 270 (2003) 342–349.
[15] D.G. Breckenridge, M. Stojanovic, R.C. Marcellus, G.C. Shore, Caspase cleavage product of BAP31 induces mitochondrial fission through endoplasmic reticulum calcium signals, enhancing cytochrome c release to the cytosol, J. Cell Biol. 160 (2003) 1115–1127.
[16] D.G. Breckenridge, M. Nguyen, S. Kuppig, M. Reth, G.C. Shore, The procaspase-8 isoform, procaspase-8L, recruited to the BAP31 complex at the endoplasmic reticulum, Proc. Natl. Acad. Sci. U.S.A. 99 (2002) 4331–4336.
[17] D.J. Granville, C.M. Carthy, H. Jiang, G.C. Shore, B.M. McManus, D.W. Hunt, Rapid cytochrome c release, activation of caspases 3, 6, 7 and 8 followed by Bap31 cleavage in HeLa cells treated with photodynamic therapy, FEBS Lett. 437 (1998) 5–10.
[18] T. Hidvegi, B.Z. Schmidt, P. Hale, D.H. Perlmutter, Accumulation of mutant alpha1-antitrypsin Z in the endoplasmic reticulum activates caspases-4 and -12, NFkappaB, and BAP31 but not the unfolded protein response, J. Biol. Chem. 280 (2005) 39002–39015.
[19] X.D. Li, H. Lankinen, N. Putkuri, O. Vapalahti, A. Vaheri, Tula hantavirus triggers pro-apoptotic signals of ER stress in Vero E6 cells, Virology 333 (2005) 180–189.
[20] N. Liu, V.L. Scofield, W. Qiang, M. Yan, X. Kuang, P.K. Wong, Interaction between endoplasmic reticulum stress and caspase 8 activation in retrovirus MoMuLV-ts1-infected astrocytes, Virology 348 (2006) 398–405.
[21] T. Iizaka, M. Tsuji, H. Oyamada, Y. Morio, K. Oguchi, Interaction between caspase-8 activation and endoplasmic reticulum stress in glycochenodeoxycholic acid-induced apoptotic HepG2 cells, Toxicology 241 (2007) 146–156.
[22] D. Chandra, G. Choy, X. Deng, B. Bhatia, P. Daniel, D.G. Tang, Association of active caspase 8 with the mitochondrial membrane during apoptosis: potential roles in cleaving BAP31 and caspase 3 and mediating mitochondrion-endoplasmic reticulum cross talk in etoposide-induced cell death, Mol. Cell. Biol. 24 (2004) 6592–6607.
[23] E. Gyan, E. Frisan, O. Beyne-Rauzy, J.C. Deschemin, C. Pierre-Eugene, C. Randriamampita, A. Dubart-Kupperschmitt, C. Garrido, F. Dreyfus, P. Mayeux, C. Lacombe, E. Solary, M. Fontenay, Spontaneous and Fas-induced apoptosis of low-grade MDS erythroid precursors involves the endoplasmic reticulum, Leukemia 22 (2008) 1864–1873.
[24] J.A. Regan, L.A. Laimins, Bap31 is a novel target of the human papillomavirus E5 protein, J. Virol. 82 (2008) 10042–10051.
[25] R. Iwasawa, A.L. Mahul-Mellier, C. Datler, E. Pazarentzos, S. Grimm, Fis1 and Bap31 bridge the mitochondria-ER interface to establish a platform for apoptosis induction, EMBO J. 30 (2011) 556–568.
[26] A. Burgeiro, C. Gajate, H. Dakir el, J.A. Villa-Pulgarin, P.J. Oliveira, F. Mollinedo, Involvement of mitochondrial and B-RAF/ERK signaling pathways in berberine-induced apoptosis in human melanoma cells, Anticancer Drugs 22 (2011) 507–518.
[27] H.M. Heath-Engel, G.C. Shore, Mitochondrial membrane dynamics, cristae remodelling and apoptosis, Biochim. Biophys. Acta 1763 (2006) 549–560.
[28] N.N. Danial, S.J. Korsmeyer, Cell death: critical control points, Cell 116 (2004) 205–219.
[29] D. Brenner, T.W. Mak, Mitochondrial cell death effectors, Curr. Opin. Cell Biol. 21 (2009) 871–877.
[30] J.E. Chipuk, T. Moldoveanu, F. Llambi, M.J. Parsons, D.R. Green, The BCL-2 family reunion, Mol. Cell 37 (2010) 299–310.
[31] H.M. Heath-Engel, N.C. Chang, G.C. Shore, The endoplasmic reticulum in apoptosis and autophagy: role of the BCL-2 protein family, Oncogene 27 (2008) 6419–6433.
[32] C.W. Distelhorst, M.D. Bootman, Bcl-2 interaction with the inositol 1,4,5-trisphosphate receptor: Role in Ca(2+) signaling and disease, Cell Calcium 50 (2011) 234–241.
[33] D. Rodriguez, D. Rojas-Rivera, C. Hetz, Integrating stress signals at the endoplasmic reticulum: the BCL-2 protein family rheostat, Biochim. Biophys. Acta 1813 (2011) 564–574.

[34] M. Germain, J.P. Mathai, H.M. McBride, G.C. Shore, Endoplasmic reticulum BIK initiates DRP1-regulated remodelling of mitochondrial cristae during apoptosis, EMBO J. 24 (2005) 1546–1556.
[35] J.P. Mathai, M. Germain, G.C. Shore, BH3-only BIK regulates BAX, BAK-dependent release of Ca2+ from endoplasmic reticulum stores and mitochondrial apoptosis during stress-induced cell death, J. Biol. Chem. 280 (2005) 23829–23836.
[36] K. Degenhardt, R. Sundararajan, T. Lindsten, C. Thompson, E. White, Bax and Bak Independently Promote Cytochrome c Release from Mitochondria, vol. 277, 2002, pp. 14127–14134.
[37] J.P. Mathai, M. Germain, R.C. Marcellus, G.C. Shore, Induction and endoplasmic reticulum location of BIK/NBK in response to apoptotic signaling by E1A and p53, Oncogene 21 (2002) 2534–2544.
[38] F.W. Ng, M. Nguyen, T. Kwan, P.E. Branton, D.W. Nicholson, J.A. Cromlish, G.C. Shore, p28 Bap31, a Bcl-2/Bcl-XL- and procaspase-8-associated protein in the endoplasmic reticulum, J. Cell Biol. 139 (1997) 327–338.
[39] W. Zhu, A. Cowie, G.W. Wasfy, L.Z. Penn, B. Leber, D.W. Andrews, Bcl-2 mutants with restricted subcellular location reveal spatially distinct pathways for apoptosis in different cell types, EMBO J. 15 (1996) 4130–4141.
[40] W.S. Rasband, ImageJ, U.S. National Institutes of Health, Bethesda, Maryland, USA, http://imagej.nih.gov/ij/, in, 1997–2011.
[41] E.L. Snapp, R.S. Hegde, M. Francolini, F. Lombardo, S. Colombo, E. Pedrazzini, N. Borgese, J. Lippincott-Schwartz, Formation of stacked ER cisternae by low affinity protein interactions, J. Cell Biol. 163 (2003) 257–269.
[42] Y. Tsujimoto, S. Shimizu, Y. Eguchi, W. Kamiike, H. Matsuda, Bcl-2 and Bcl-xL block apoptosis as well as necrosis: possible involvement of common mediators in apoptotic and necrotic signal transduction pathways, Leukemia 11 (Suppl 3) (1997) 380–382.
[43] G.P. Amarante-Mendes, D.M. Finucane, S.J. Martin, T.G. Cotter, G.S. Salvesen, D.R. Green, Anti-apoptotic oncogenes prevent caspase-dependent and independent commitment for cell death, Cell Death Differ. 5 (1998) 298–306.
[44] K. Fukuda, M. Yamamoto, Acquisition of resistance to apoptosis and necrosis by Bcl-xL over-expression in rat hepatoma McA-RH8994 cells, J. Gastroenterol. Hepatol. 14 (1999) 682–690.
[45] M. Haraguchi, S. Torii, S. Matsuzawa, Z. Xie, S. Kitada, S. Krajewski, H. Yoshida, T.W. Mak, J.C. Reed, Apoptotic protease activating factor 1 (Apaf-1)-independent cell death suppression by Bcl-2, J. Exp. Med. 191 (2000) 1709–1720.
[46] B. Single, M. Leist, P. Nicotera, Differential effects of bcl-2 on cell death triggered under ATP-depleting conditions, Exp. Cell Res. 262 (2001) 8–16.
[47] G. Denecker, D. Vercammen, M. Steemans, T. Vanden Berghe, G. Brouckaert, G. Van Loo, B. Zhivotovsky, W. Fiers, J. Grooten, W. Declercq, P. Vandenabeele, Death receptor-induced apoptotic and necrotic cell death: differential role of caspases and mitochondria, Cell Death Differ. 8 (2001) 829–840.
[48] J. Saldeen, Cytokines induce both necrosis and apoptosis via a common Bcl-2-inhibitable pathway in rat insulin-producing cells, Endocrinology 141 (2000) 2003–2010.
[49] J. Fombonne, S. Reix, R. Rasolonjanahary, E. Danty, S. Thirion, G. Laforge-Anglade, O. Bosler, P. Mehlen, A. Enjalbert, S. Krantic, Epidermal growth factor triggers an original, caspase-independent pituitary cell death with heterogeneous phenotype, Mol. Biol. Cell 15 (2004) 4938–4948.
[50] K.F. Sung, I.V. Odinokova, O.A. Mareninova, Z. Rakonczay Jr., P. Hegyi, S.J. Pandol, I. Gukovsky, A.S. Gukovskaya, Prosurvival Bcl-2 proteins stabilize pancreatic mitochondria and protect against necrosis in experimental pancreatitis, Exp. Cell Res. 315 (2009) 1975–1989.
[51] J. Fombonne, L. Padron, A. Enjalbert, S. Krantic, A. Torriglia, A novel paraptosis pathway involving LEI/L-DNaseII for EGF-induced cell death in somato-lactotrope pituitary cells, Apoptosis 11 (2006) 367–375.
[52] A.M. Petros, E.T. Olejniczak, S.W. Fesik, Structural biology of the Bcl-2 family of proteins, Biochim. Biophys. Acta 1644 (2004) 83–94.
[53] J.K. Brunelle, A. Letai, Control of mitochondrial apoptosis by the Bcl-2 family, J. Cell Sci. 122 (2009) 437–441.
[54] T. Oltersdorf, S.W. Elmore, A.R. Shoemaker, R.C. Armstrong, D.J. Augeri, B.A. Belli, M. Bruncko, T.L. Deckwerth, J. Dinges, P.J. Hajduk, M.K. Joseph, S. Kitada, S.J. Korsmeyer, A.R. Kunzer, A. Letai, C. Li, M.J. Mitten, D.G. Nettesheim, S. Ng, P.M. Nimmer, J.M. O'Connor, A. Oleksijew, A.M. Petros, J.C. Reed, W. Shen, S.K. Tahir, C.B. Thompson, K.J. Tomaselli, B. Wang, M.D. Wendt, H. Zhang, S.W. Fesik, S.H. Rosenberg, An inhibitor of Bcl-2 family proteins induces regression of solid tumours, Nature 435 (2005) 677–681.
[55] B. Leber, F. Geng, J. Kale, D.W. Andrews, Drugs targeting Bcl-2 family members as an emerging strategy in cancer, Expert Rev. Mol. Med. 12 (2010) e28.
[56] S.A. Oakes, L. Scorrano, J.T. Opferman, M.C. Bassik, M. Nishino, T. Pozzan, S.J. Korsmeyer, Proapoptotic BAX and BAK regulate the type 1 inositol trisphosphate receptor and calcium leak from the endoplasmic reticulum, Proc. Natl. Acad. Sci. U.S.A. 102 (2005) 105–110.
[57] Y.P. Rong, G. Bultynck, A.S. Aromolaran, F. Zhong, J.B. Parys, H. De Smedt, G.A. Mignery, H.L. Roderick, M.D. Bootman, C.W. Distelhorst, The BH4 domain of Bcl-2 inhibits ER calcium release and apoptosis by binding the regulatory and coupling domain of the IP3 receptor, Proc. Natl. Acad. Sci. U.S.A. 106 (2009) 14397–14402.
[58] P. Pinton, D. Ferrari, P. Magalhaes, K. Schulze-Osthoff, F. Di Virgilio, T. Pozzan, R. Rizzuto, Reduced loading of intracellular Ca(2+) stores and downregulation of capacitative Ca(2+) influx in Bcl-2-overexpressing cells, J. Cell Biol. 148 (2000) 857–862.
[59] R. Foyouzi-Youssefi, S. Arnaudeau, C. Borner, W.L. Kelley, J. Tschopp, D.P. Lew, N. Demaurex, K.H. Krause, Bcl-2 decreases the free Ca2+ concentration within the endoplasmic reticulum, Proc. Natl. Acad. Sci. U.S.A. 97 (2000) 5723–5728.
[60] A.E. Palmer, C. Jin, J.C. Reed, R.Y. Tsien, Bcl-2-mediated alterations in endoplasmic reticulum Ca2+ analyzed with an improved genetically encoded fluorescent sensor, Proc. Natl. Acad. Sci. U.S.A. 101 (2004) 17404–17409.
[61] J. Hacki, L. Egger, L. Monney, S. Conus, T. Rosse, I. Fellay, C. Borner, Apoptotic crosstalk between the endoplasmic reticulum and mitochondria controlled by Bcl-2, Oncogene 19 (2000) 2286–2295.
[62] M. Hirabayashi, K. Inoue, K. Tanaka, K. Nakadate, Y. Ohsawa, Y. Kamei, A.H. Popiel, A. Sinohara, A. Iwamatsu, Y. Kimura, Y. Uchiyama, S. Hori, A. Kakizuka, VCP/p97 in abnormal protein aggregates, cytoplasmic vacuoles, and cell death, phenotypes relevant to neurodegeneration, Cell Death Differ. 8 (2001) 977–984.
[63] M. Nagahama, M. Suzuki, Y. Hamada, K. Hatsuzawa, K. Tani, A. Yamamoto, M. Tagaya, SVIP is a novel VCP/p97-interacting protein whose expression causes cell vacuolation, Mol. Biol. Cell 14 (2003) 262–273.
[64] E.G. Mimnaugh, W. Xu, M. Vos, X. Yuan, J.S. Isaacs, K.S. Bisht, D. Gius, L. Neckers, Simultaneous inhibition of hsp 90 and the proteasome promotes protein ubiquitination, causes endoplasmic reticulum-derived cytosolic vacuolization, and enhances antitumor activity, Mol. Cancer Ther. 3 (2004) 551–566.
[65] C. Wojcik, M. Yano, G.N. DeMartino, RNA interference of valosin-containing protein (VCP/p97) reveals multiple cellular roles linked to ubiquitin/proteasome-dependent proteolysis, J. Cell Sci. 117 (2004) 281–292.
[66] S.T. Nawrocki, J.S. Carew, K. Dunner Jr., L.H. Boise, P.J. Chiao, P. Huang, J.L. Abbruzzese, D.J. McConkey, Bortezomib inhibits PKR-like endoplasmic reticulum (ER) kinase and induces apoptosis via ER stress in human pancreatic cancer cells, Cancer Res. 65 (2005) 11510–11519.
[67] M. Noguchi, T. Takata, Y. Kimura, A. Manno, K. Murakami, M. Koike, H. Ohizumi, S. Hori, A. Kakizuka, ATPase activity of p97/valosin-containing protein is regulated by oxidative modification of the evolutionally conserved cysteine 522 residue in Walker A motif, J. Biol. Chem. 280 (2005) 41332–41341.
[68] E.G. Mimnaugh, W. Xu, M. Vos, X. Yuan, L. Neckers, Endoplasmic reticulum vacuolization and valosin-containing protein relocalization result from simultaneous hsp90 inhibition by geldanamycin and proteasome inhibition by velcade, Mol. Cancer Res. 4 (2006) 667–681.
[69] C. Wojcik, M. Rowicka, A. Kudlicki, D. Nowis, E. McConnell, M. Kujawa, G.N. DeMartino, Valosin-containing protein (p97) is a regulator of endoplasmic reticulum stress and of the degradation of N-end rule and ubiquitin-fusion degradation pathway substrates in mammalian cells, Mol. Biol. Cell 17 (2006) 4606–4618.
[70] W.X. Ding, H.M. Ni, X.M. Yin, Absence of Bax switched MG132-induced apoptosis to non-apoptotic cell death that could be suppressed by transcriptional or translational inhibition, Apoptosis 12 (2007) 2233–2244.
[71] Y. Ustundag, S.F. Bronk, G.J. Gores, Proteasome inhibition-induces endoplasmic reticulum dysfunction and cell death of human cholangiocarcinoma cells, World J. Gastroenterol. 13 (2007) 851–857.
[72] C. Denoyelle, G. Abou-Rjaily, V. Bezrookove, M. Verhaegen, T.M. Johnson, D.R. Fullen, J.N. Pointer, S.B. Gruber, L.D. Su, M.A. Nikiforov, R.J. Kaufman, B.C. Bastian, M.S. Soengas, Anti-oncogenic role of the endoplasmic reticulum differentially activated by mutations in the MAPK pathway, Nat. Cell Biol. 8 (2006) 1053–1063.
[73] R. Kar, P.K. Singha, M.A. Venkatachalam, P. Saikumar, A novel role for MAP1 LC3 in nonautophagic cytoplasmic vacuolation death of cancer cells, Oncogene 28 (2009) 2556–2568.
[74] S. Tardito, C. Isella, E. Medico, L. Marchio, E. Bevilacqua, M. Hatzoglou, O. Bussolati, R. Franchi-Gazzola, The thioxotriazole copper(II) complex A0 induces endoplasmic reticulum stress and paraptotic death in human cancer cells, J. Biol. Chem. 284 (2009) 24306–24319.
[75] G.E. Breitwieser, J.C. McLenithan, J.F. Cortese, J.M. Shields, M.M. Oliva, J.L. Majewski, C.E. Machamer, V.W. Yang, Colonic epithelium-enriched protein A4 is a proteolipid that exhibits ion channel characteristics, Am. J. Physiol. 272 (1997) C957–C965.
[76] S. Sperandio, I. de Belle, D.E. Bredesen, An alternative, nonapoptotic form of programmed cell death, Proc. Natl. Acad. Sci. U.S.A. 97 (2000) 14376–14381.
[77] S. Castro-Obregon, G. Del Rio, S.F. Chen, R.A. Swanson, H. Frankowski, R.V. Rao, V. Stoka, S. Vesce, D.G. Nicholls, D.E. Bredesen, A ligand-receptor pair that triggers a non-apoptotic form of programmed cell death, Cell Death Differ. 9 (2002) 807–817.
[78] S. Tardito, O. Bussolati, F. Gaccioli, R. Gatti, S. Guizzardi, J. Uggeri, L. Marchio, M. Lanfranchi, R. Franchi-Gazzola, Non-apoptotic programmed cell death induced by a copper(II) complex in human fibrosarcoma cells, Histochem. Cell Biol. 126 (2006) 473–482.
[79] N. Hoa, M.P. Myers, T.G. Douglass, J.G. Zhang, C. Delgado, L. Driggers, L.L. Callahan, G. VanDeusen, J.T. Pham, N. Bhakta, L. Ge, M.R. Jadus, Molecular mechanisms of paraptosis induction: implications for a non-genetically modified tumor vaccine, PLoS One 4 (2009) e4631.
[80] Q. Sun, T. Chen, X. Wang, X. Wei, Taxol induces paraptosis independent of both protein synthesis and MAPK pathway, J. Cell. Physiol. 222 (2010) 421–432.
[81] S. Tardito, I. Bassanetti, C. Bignardi, L. Elviri, M. Tegoni, C. Mucchino, O. Bussolati, R. Franchi-Gazzola, L. Marchio, Copper binding agents acting as copper ionophores lead to caspase inhibition and paraptotic cell death in human cancer cells, J. Am. Chem. Soc. 133 (2011) 6235–6242.
[82] S. Sperandio, K.S. Poksay, B. Schilling, D. Crippen, B.W. Gibson, D.E. Bredesen, Identification of new modulators and protein alterations in non-apoptotic programmed cell death, J. Cell. Biochem. 111 (2010) 1401–1412.
[83] M.J. Yoon, E.H. Kim, J.H. Lim, T.K. Kwon, K.S. Choi, Superoxide anion and proteasomal dysfunction contribute to curcumin-induced paraptosis of malignant breast cancer cells, Free Radic. Biol. Med. 48 (2010) 713–726.
[84] G. Kroemer, L. Galluzzi, P. Vandenabeele, J. Abrams, E.S. Alnemri, E.H. Baehrecke, M.V. Blagosklonny, W.S. El-Deiry, P. Golstein, D.R. Green, M. Hengartner, R.A. Knight, S. Kumar, S.A. Lipton, W. Malorni, G. Nunez, M.E. Peter, J. Tschopp, J.

Yuan, M. Piacentini, B. Zhivotovsky, G. Melino, Classification of cell death: recommendations of the Nomenclature Committee on Cell Death 2009, Cell Death Differ. 16 (2009) 3–11.
[85] S.T. Nawrocki, J.S. Carew, M.S. Pino, R.A. Highshaw, K. Dunner Jr., P. Huang, J.L. Abbruzzese, D.J. McConkey, Bortezomib sensitizes pancreatic cancer cells to endoplasmic reticulum stress-mediated apoptosis, Cancer Res. 65 (2005) 11658–11666.
[86] L. Scorrano, S.A. Oakes, J.T. Opferman, E.H. Cheng, M.D. Sorcinelli, T. Pozzan, S.J. Korsmeyer, BAX and BAK regulation of endoplasmic reticulum Ca2+: a control point for apoptosis, Science 300 (2003) 135–139.
[87] G. Kroemer, S.J. Martin, Caspase-independent cell death, Nat. Med. 11 (2005) 725–730.
[88] S.W. Tait, D.R. Green, Caspase-independent cell death: leaving the set without the final cut, Oncogene 27 (2008) 6452–6461.